Metal Sensing by a Glycine-Histidine Repeat Sequence Regulates the Heme Degradation Activity of PM0042 from *Pasteurella multocida*

Takeshi Uchida*, Kazuki Ota, Akinobu Tatsumi, Syota Takeuchi, and Koichiro Ishimori

***Corresponding Author**
Department of Chemistry, Faculty of Science, Hokkaido University, Sapporo 060-0810, Japan.
uchida@sci.hokudai.ac.jp (T. Uchida).

ABSTRACT: PM0042 protein from the gram-negative bacterial pathogen *Pasteurella multocida* is homologous to the heme-degrading enzyme HutZ belonging to the pyridoxine-5-phosphate oxidase-like family. A characteristic feature of PM0042 is possession of a glycine-histidine (GH) repeat sequence at the C-terminal region. In this study, we examined the heme degradation ability of PM0042, with particular focus on the role of the GH repeat sequence. PM0042 was expressed in *Escherichia coli* and successfully purified using a nickel (Ni^{2+})-affinity column without a histidine tag, suggesting that its GH motif facilitates binding to Ni^{2+}. Reaction with ascorbic acid induced a significant decrease in the Soret band, suggesting breakage of heme. While a Fe^{2+}-ferrozine complex was not formed upon addition of ferrozine to the solution after the reaction, prior addition of metal ions to fill the metal binding site in the GH repeat sequence led to increased complex formation. In the presence of Fe^{2+}, the heme degradation rate was accelerated ~3-fold, supporting the theory that Fe^{2+} binds the PM0042 protein (possibly at the GH repeat sequence) and enhances its heme degradation activity. In contrast to HutZ from *Vibrio cholerae* in which enzymatic activity is regulated by protonation status of the heme proximal ligand, heme reduction is not the rate-determining step for PM0042. Rather, proton transfer to reduced oxy-heme is affected, as established with the H_2O/D_2O isotope experiment. Based on the collective findings, the GH repeat sequence of PM0042 is proposed to function as a metal sensor that modulates iron uptake via the heme-degrading process in *Pasteurella multocida*.

INTRODUCTION

HutZ from *Vibrio cholerae* (*Vc*HutZ), a heme-degrading enzyme, produces biliverdin, Fe^{2+} and carbon monoxide via reaction with ascorbic acid.[1–3] *Vc*HutZ-mediated heme degradation is characteristically dependent on pH.[1,3] The amount of Fe^{2+} released from heme has been previously determined using ferrozine, a strong chelator of ferrous ions.[4,5] Data from plots of Fe^{2+}-ferrozine complex against pH suggest that *Vc*HutZ degrades ~90% heme at pH 6.0 but only ~5% at pH 8.0 and is almost inactive at pH >8.0.[3] Based on reduction of heme being the initial step of heme degradation, the heme reduction rate at pH 6.0 was reported to be ~3-fold larger than that at pH 8.0, supporting the theory that the initial heme degradation step is accelerated at pH 6.0, thus leading to higher activity. In addition to heme reduction rates, the absorption spectra of heme-*Vc*HutZ are different between pH 6.0 and 8.0.[1] The heme-*Vc*HutZ complex is a mixture of high-spin (Fe^{3+}–H_2O) and low-spin (Fe^{3+}–OH^-) states. The ratio of high-spin/low-spin heme is also correlated with pH. Specifically, high-spin heme is dominant at low pH and low-spin heme at high pH and may therefore be correlated with the heme degradation activity of *Vc*HutZ.

The pH-dependent spin state changes are related to protein conformational changes. *Vc*HutZ is a dimeric protein distinct from its mammalian counterpart, the monomeric heme oxygenase (HO). Earlier fluorescence resonance energy transfer (FRET) measurements have demonstrated pH-dependent modulation of subunit-subunit interactions of *Vc*HutZ.[3] The distance between heme and sole tryptophan located near the proximal site of heme is changed to <2 Å upon lowering pH. A heme axial ligand of *Vc*HutZ, His170, putatively forms a proximal hydrogen bond with nearby Asp132,[6] a common feature of heme peroxidases.[7–9] However, the hydrogen bond partner of the axial heme ligand of *Vc*HutZ is acquired from a different subunit, which is a unique characteristic. Thus, small but distinct alterations in distance between heme and Trp109 with pH changes are sufficient to modulate the strength of proximal hydrogen bonding.

To validate these characteristics of the HugZ family, our group conducted a BLAST search. Among the proteins homologous to *Vc*HutZ, we detected a characteristic sequence in those from *Pasteurella multocida*, a gram-negative bacterial pathogen responsible for a number of important animal diseases, including fowl cholera.[10] BLAST analysis revealed sequence homology of 77% between PM0042 and *Vc*HutZ (Figure S1), supporting a potentially similar heme degradation function of PM0042. Interestingly, the amino acid sequence of PM0042 contains a glycine-histidine (GH) repeat sequence at the C-terminus (Figure S1).

In the current study, we investigated the heme degradation ability of PM0042, focusing on the potential role of the C-terminal GH repeat motif in this function. Our experiments showed that PM0042 degrades heme via reaction with ascorbic acid, with greater enzymatic activity at pH 6.0 than pH 8.0, as observed for *Vc*HutZ. Interestingly, PM0042 bound the Ni^{2+}-affinity column in the absence of a histidine tag, raising the possibility that the GH motif traps iron released from disrupted heme. Prior addition of Fe^{2+} to the reaction solution of PM0042 to occupy the metal binding sites enhanced the heme degradation reaction by ~3-fold, which was not observed with other divalent metal cations, such as Ni^{2+} and Zn^{2+}. The collective findings clearly support a function of the GH repeat sequence as a sensor of the concentration of Fe^{2+} that modulates the activity of PM0042 to acquire Fe^{2+} from heme.

RESULTS

Cloning, Expression, Purification, and Heme Binding of PM0042. PM0042 from *P. multocida* was overexpressed in *E. coli* strain BL21(DE3). The protein was designed for expression without a His_6 tag, but successfully purified using a HisTrap nickel affinity column through an endogenous histidine cluster. Purified protein was verified via SDS-PAGE (~95% purity) and migrated as a single band with a molecular mass of ~20 kDa (Figure 1A), in agreement with the

calculated molecular mass of PM0042 (20.7 kDa). Size-exclusion chromatography analysis revealed a large peak at 83.9 mL (Figure 1B) corresponding to a molecular mass of ~40 kDa based on protein molecular mass standards. The data suggest that PM0042 exists as a dimer, as observed for HutZ from *V. cholerae* (*Vc*HutZ).[1]

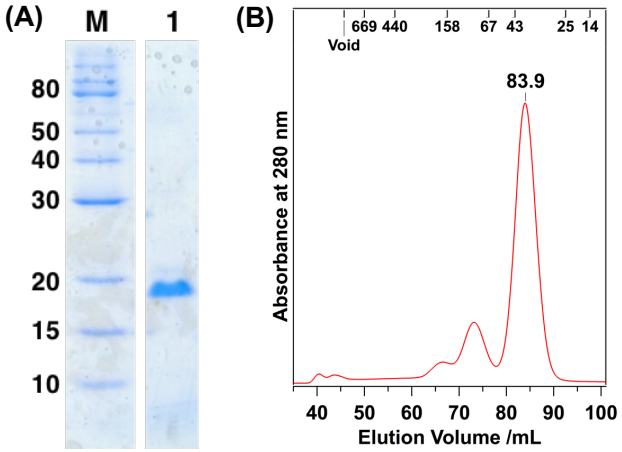

Figure 1. Purification of PM0042**.** (A) SDS-PAGE of purified PM0042 (Lane 1) and molecular mass markers (Lane M). (B) Determination of the molecular mass of PM0042 via size exclusion chromatography. Analytical gel filtration was performed using a Superdex 200pg column equilibrated with 50 mM Tris-HCl and 150 mM NaCl (pH 8.0) at a flow rate of 1 mL min^{-1}. The protein standards used were as follows: ribonuclease A (13.7 kDa), chymotrypsinogen A (25 kDa), ovalbumin (43 kDa), bovine serum albumin (67 kDa), aldolase (158 kDa), ferritin (440 kDa), thyrogloblin (669 kDa), and blue dextran (2000 kDa).

The purified protein was colorless, suggesting no endogenous heme content after purification. Upon addition of an aliquot of hemin to purified protein, a spectrum with a sharp band centered at 413 nm distinct from that of free hemin (387 nm, Figure 2A) was obtained, indicating specific binding of PM0042 to heme. The heme-binding ability of PM0042 was confirmed by determining the stoichiometry and binding constant values upon titration of a fixed concentration of PM0042 solution with heme. Difference spectra of PM0042 minus buffer titrated with the same amount of heme are presented in Figure 2B. Data from a plot of the absorbance difference at 416 nm against heme concentration (Figure 2B, inset) suggest that PM0042 binds one equivalent of heme. On the

basis of pyridine hemochrome spectra of the sample, stoichiometry of heme binding to PM0042 was consistently determined as 1:1. The apparent dissociation constant ($K_{d,heme}$) was calculated as 0.26 ± 0.06 μM by fitting the absorbance difference to Equation 1.

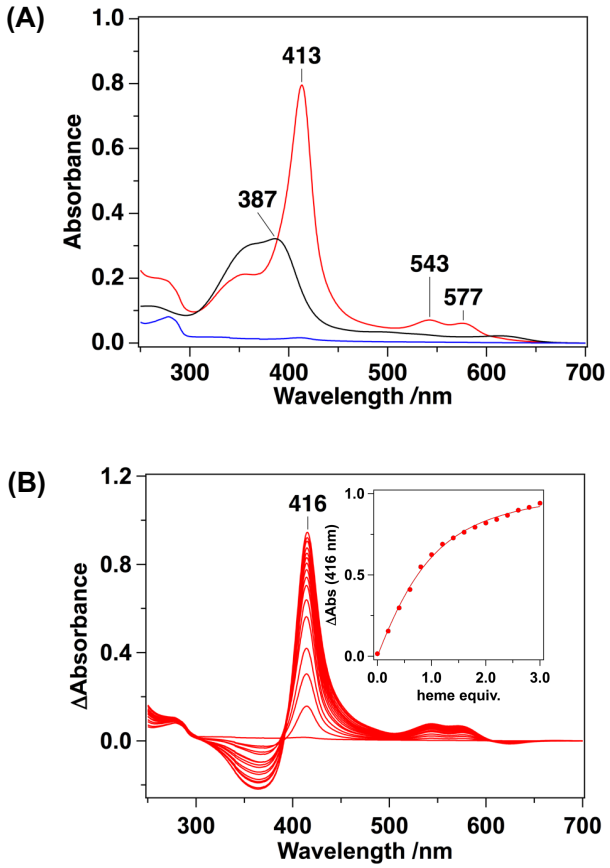

Figure 2. Absorption spectra of heme titration. (A) Absorption spectra of purified PM0042 protein (blue line), heme (black line), and heme complexed with PM0042 (red line). (B) Absorption difference spectra of heme-PM0042. (Inset) Differences at 416 nm following incremental addition of heme (1–30 μM) to PM0042 (10 μM) in 50 mM Tris-HCl and 150 mM NaCl (pH 8.0) relative to a blank cell sample containing buffer alone.

Heme degradation activity of PM0042. Following confirmation of heme binding to PM0042, the heme degradation reaction was initially monitored using ascorbic acid as an electron source. The reaction was conducted in the presence of catalase to decompose H_2O_2 produced by the reduction of molecular oxygen by ascorbic acid. Spectral changes induced by the addition of

ascorbic acid at pH 8.0 are presented in Figure 3A. The Soret band decreased by ~25% after the reaction, suggesting limited heme degradation under these conditions.[11] The heme degradation reaction of *Vc*HutZ with ascorbic acid is reported to be dependent on pH. In view of the earlier finding that limited heme is degraded by *Vc*HutZ at pH >8.0, while the reaction is significantly accelerated at pH 6.0,[1,3] the same experiment was conducted for PM0042 at pH 6.0. As expected, lowering the pH from 8.0 to 6.0 led to a decrease in the Soret band and increased weak broad absorption in the 700–800 nm region (Figure 3B), indicating that PM0042 effectively degrades heme using ascorbic acid as an electron source and is more active at lower pH, analogous to *Vc*HutZ.

To quantify Fe^{2+} release accompanying heme degradation, we added ferrozine, which forms a red-colored complex with Fe^{2+},[4,5] to the final reaction solution. To avoid possible ferrozine-induced inhibition of heme degradation,[12] ferrozine was added after the reaction. Absorbance at 562 nm corresponding to the Fe^{2+}-ferrozine complex did not appear even 60 min after the reaction (Figure 3A, B) and the estimated yield of Fe^{2+} released from heme was <5%. The unexpected result clearly indicates that Fe^{2+} is not released from heme, which is not consistent with the observed significant decrease in the Soret band.

To further confirm the heme degradation ability of PM0042, H_2O_2 was used as an electron source. In the reactions of mammalian heme oxygenase[13–15] and *Vc*HutZ[1] with H_2O_2, verdoheme, a key intermediate in the heme degradation reaction, is formed. Upon reaction of heme-PM0042 with H_2O_2, absorbance at 656 nm increased at pH 8.0 (Figure 3C) and that at 654 nm at pH 6.0 (Figure 3D). The ratio of the height of the 654–656 nm band of verdoheme to the Soret band of ferric heme at pH 8.0 and 6.0 was 0.1266 and 0.1477, respectively, which correspond to ~104% and 81% for *Vc*HutZ (0.1221for pH 8.0 and 0.1816 for pH 6.0), respectively.[1,2] The appearance of the 654–656 nm band signifies the formation of verdoheme in the reaction of H_2O_2 with PM0042. After the reaction with H_2O_2, heme was extracted by a solid-phase column and its mass spectrum

was measured. The main peak was observed at 619.51 (Figure S2A), which corresponds to the calculated mass of verdoheme (619.46). This result also supports the formation of verdoheme.

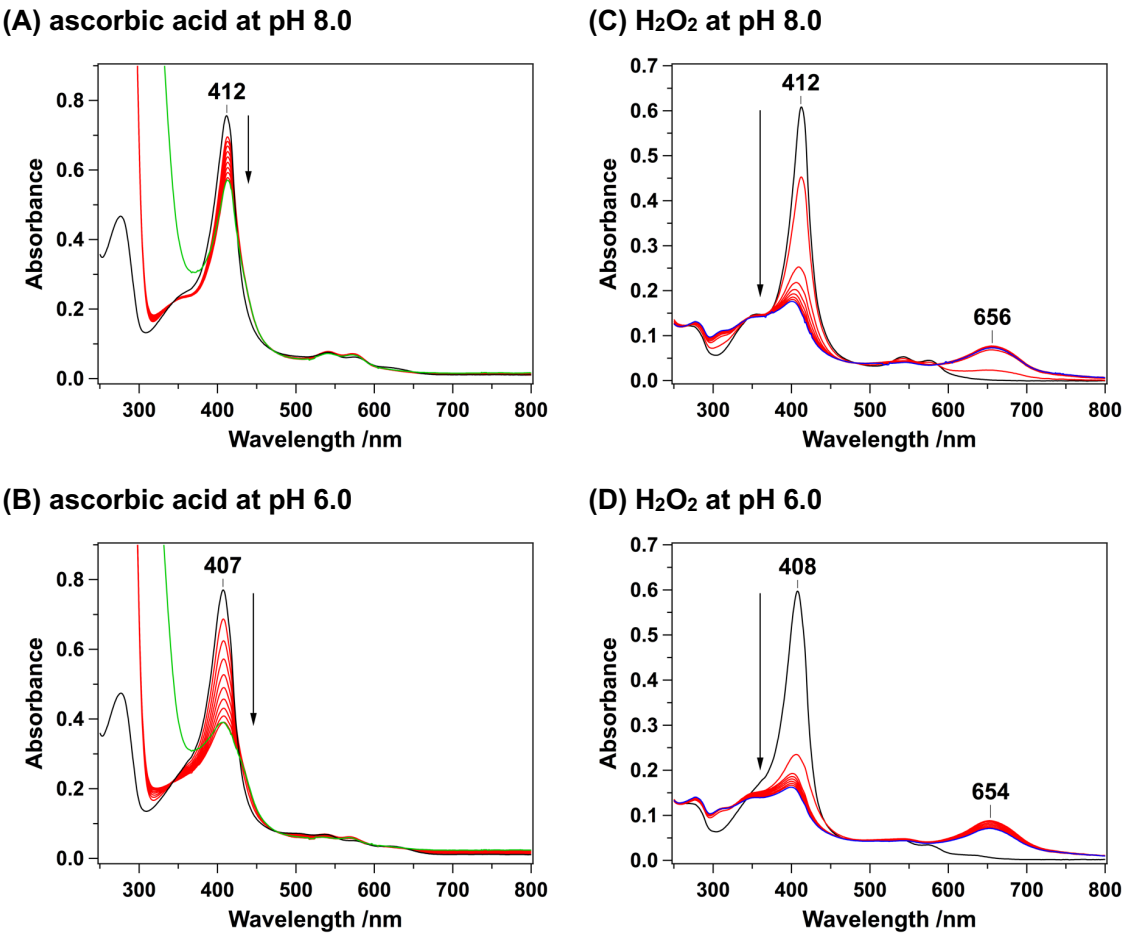

Figure 3. Heme degradation reaction of heme-PM0042 with ascorbic acid (1.0 mM) in 50 mM Tris-HCl and 150 mM NaCl at pH 8.0 (A) and 50 mM MES and 150 mM NaCl at pH 6.0 (B). Spectra were recorded before the addition of ascorbic acid (black line) and at 4 min intervals for 60 min after the addition of ascorbic acid (red line). Green line represents spectra following the addition of ferrozine 60 min after initiation of the reaction. Heme degradation reactions of heme-PM0042 mutants with H_2O_2 (0.2 mM) in 50 mM Tris-HCl and 150 mM NaCl at pH 8.0 (C) and 50 mM MES and 150 mM NaCl at pH 6.0 (D). Spectra were recorded before the addition of H_2O_2 and at 1 min intervals for 15 min after the addition of H_2O_2.

Verdoheme is not the final product of HO[15] and *Vc*HutZ[1] and further oxidation generates biliverdin.[1,15,16] To establish whether biliverdin is produced by PM0042, verdoheme was formed

by reacting PM0042 with H_2O_2, followed by treatment with ascorbic acid under aerobic conditions. Absorption at 654-657 nm of verdoheme decreased without a shift immediately after the addition of ascorbic acid at both pH 8.0 and 6.0 (Figure 4A, B). Addition of ferrozine led to a minimal or no peak at 562 nm at pH 8.0 (Figure 4A), whereas a small but distinct peak appeared at pH 6.0 (Figure 4B), indicating slight release of ferrous iron at the lower pH. Although the reaction of heme-PM0042 with ascorbic acid only did not lead to release of Fe^{2+} (Figure 3B), consecutive treatment with H_2O_2 and ascorbic acid yielded Fe^{2+} and biliverdin. The mass of the product was also measudred (Figure S2B). The peak of 583.24 corresponds to that of calculated biliverdin (582.64), indicating the formation of biliverdin. Our results indicate that PM0042 possesses the ability to degrade heme and produce Fe^{2+} and biliverdin.

Formation of biliverdin was further validated via high-performance liquid chromatography (HPLC). Reaction of free heme with ascorbic acid produces four biliverdin isomers, specifically, IXα, IXβ, IXδ and IXγ,[17] which appear at 15.5, 21.1, 23.3, and 32.7 min, respectively, in the HPLC chromatogram (Figure 4C). Peaks were assigned on the basis of a previous report.[18] In the chromatogram of PM0042, two large peaks were observed at 21.0 and 23.2 min corresponding to biliverdin IXβ and biliverdin IXδ, respectively (Figure 4C). Based on these findings, we conclude that biliverdin is produced by PM0042 via heme cleavage at the β- or δ-meso positions.

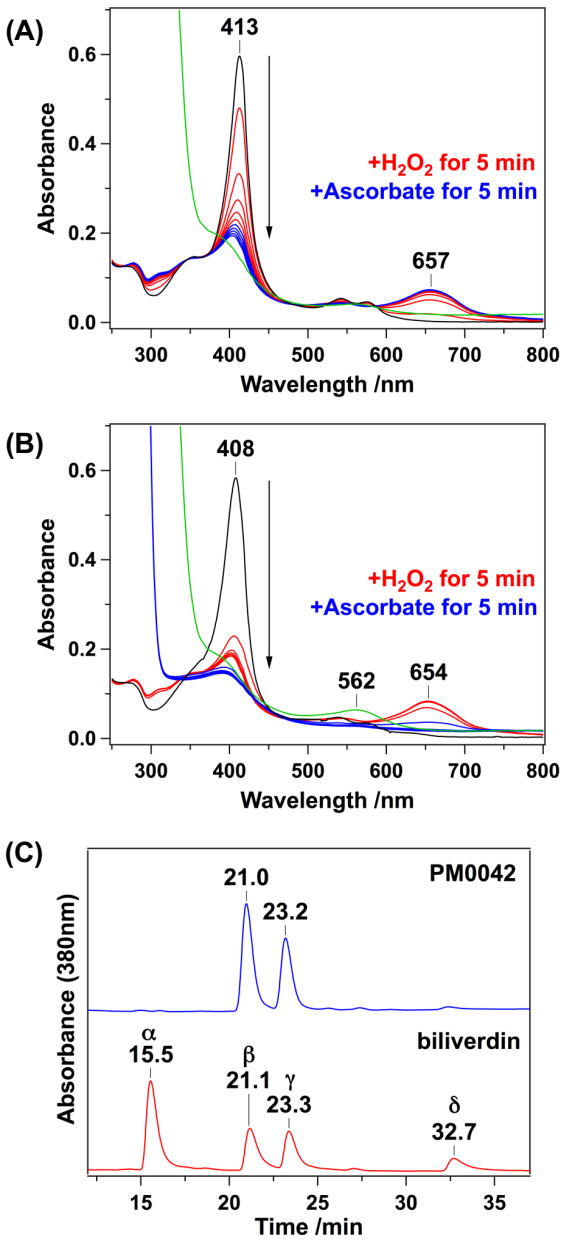

Figure 4. Heme degradation reaction of heme-PM0042 with H_2O_2 (0.2 mM) and ascorbic acid (1.0 mM) in 50 mM Tris-HCl and 150 mM NaCl at pH 8.0 (A) and 50 mM MES and 150 mM NaCl at pH 6.0 (B). Spectra were recorded before the addition of H_2O_2 and at 1 min intervals for 5 min after the addition of H_2O_2 following treatment with ascorbic acid, and again at 1 min intervals for a further 5 min. The green line represents spectra after the addition of ferrozine at the end of the reaction. (C) HPLC of products from reactions of free heme (red line) and heme-PM0042 (blue line) in 50 mM Tris-HCl and 150 mM NaCl with 0.1 mM H_2O_2 and 1 mM ascorbic acid at pH 8.0.

Heme Degradation Reaction in the Presence of Metal Ions. In view of the generation of verdoheme and biliverdin (Figures 3, 4) and significant decrease in the Soret band after reaction of PM0042 with ascorbic acid at pH 6.0, we hypothesized that Fe^{2+} is released by degradation of heme but trapped by the protein, potentially via interactions with the C-terminal GH repeat that could represent a metal binding site. To examine this theory, metal ions were added to the reaction solution in advance to occupy the binding sites on the GH repeat sequence. In the presence of 10 μM Zn^{2+} or Mn^{2+}, the amount of Fe^{2+} monitored using ferrozine was ~0%, similar to that in the absence of metal ions. However, addition of Co^{2+} or Ni^{2+} increased the ratio of the Fe^{2+}-ferrozine complex to the initial protein concentration to 36% and 31%, respectively (Figure 5A). In the presence of 10 μM Fe^{2+}, the ratio was significantly increased to 146% (Figure 5B). Although this value includes exogenous Fe^{2+}, the same reaction conducted at pH 8.0 revealed limited iron release (<5%) (Figure 5C), suggesting that addition of Fe^{2+} prior to the reaction promotes formation of the ferrozine-Fe^{2+} complex at pH 6.0. Therefore, we propose that additional metal ions bind to the GH repeat sequence to occupy the metal binding sites, resulting in increased Fe^{2+} release into the solvent where it is captured by ferrozine to form metal complexes.

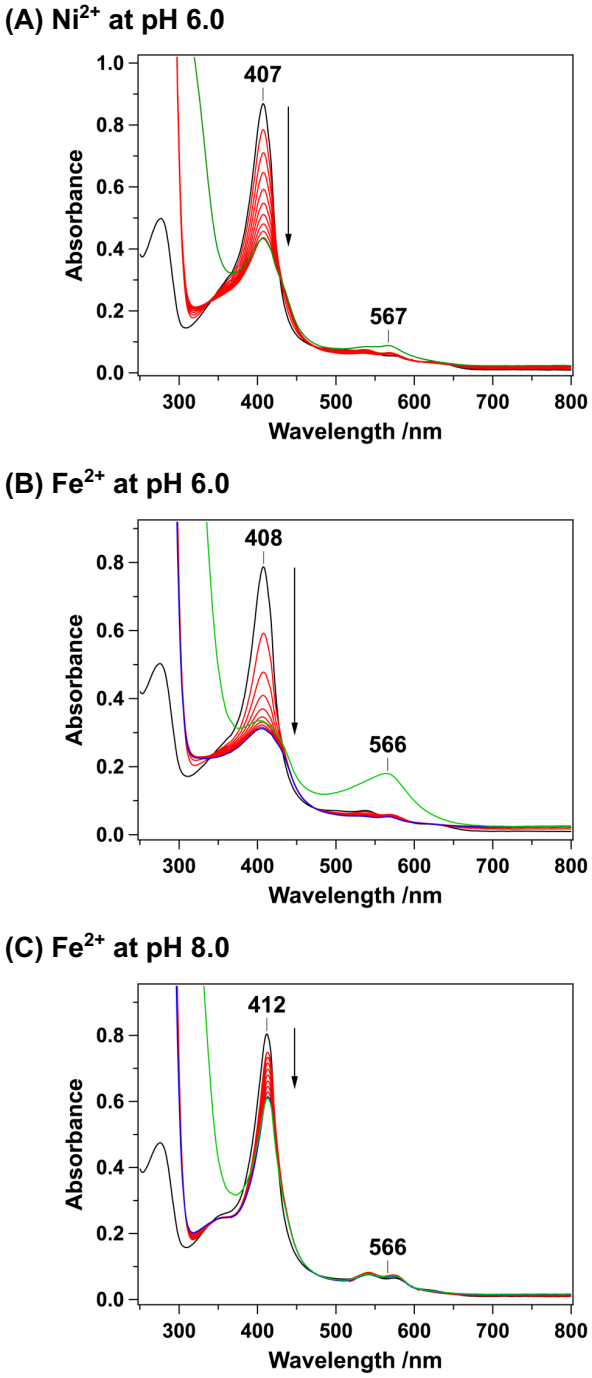

Figure 5. Heme degradation reaction of heme-PM0042 with ascorbic acid (1.0 mM) in 50 mM MES and 150 mM NaCl at pH 6.0 in the presence of (A) Ni^{2+} and (B) Fe^{2+} and 50 mM Tris-HCl and 150 mM NaCl at pH 8.0 in the presence of Fe^{2+} (C). Spectra were recorded before the addition of ascorbic acid (black line) and at 4-min intervals for 60 min after the addition of ascorbic acid (red line). The green line represents spectra following the addition of ferrozine at 60 min after initiation of the reaction.

The rates of heme degradation in the absence and presence of metal ions were further compared (Figure 6). In the presence of Co^{2+}, Ni^{2+}, Mn^{2+} or Zn^{2+}, the time-course of decrease in Soret absorption almost overlapped with that in the absence of these metals. In contrast, in the presence of Fe^{2+}, the reaction was significantly accelerated. The time-course fitted well with a single exponential function. The apparent kinetic constant k_{app} in the presence of Fe^{2+} ($4.18 \pm 0.02\ h^{-1}$) was ~3-fold larger than that in the absence of Fe^{2+} ($1.27 \pm 0.04\ h^{-1}$), indicating that Fe^{2+} is the only metal ion with a significant effect on the rate of decrease in Soret absorbance.

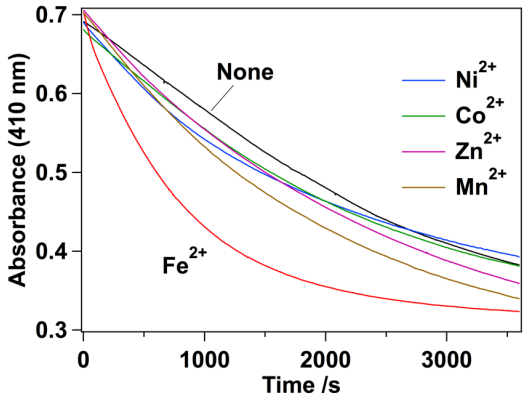

Figure 6. Time course of absorbance at 410 nm in the reaction of heme-PM0042 (10 μM) with ascorbic acid (1.0 mM) in 50 mM MES and 150 mM NaCl at pH 6.0 in the presence of Ni^{2+}, Co^{2+}, Zn^{2+}, Mn^{2+} and Fe^{2+} (30 μM) and absence of metal.

To determine the amount of Fe^{2+} required for enhancement of PM0042 activity, we compared the rates of heme degradation at various Fe^{2+} concentrations (0-4 equivalents) (Figure 7A). The decay curves were fitted to a single exponential function and rate constants plotted against Fe^{2+} concentration (Figure 7B). While this plot did not provide a clear equivalent point, the rate showed a plateau after the addition of 3 equivalents of Fe^{2+} and ~60% of the changes were reached at 1 equivalent of Fe^{2+}. Our collective data suggest that 1 or 2 molecules of Fe^{2+} interact with the GH motif.

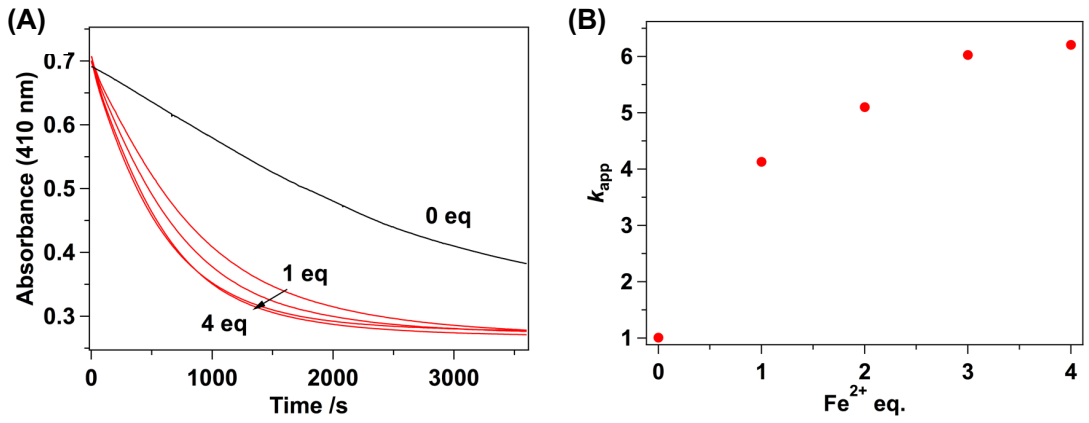

Figure 7. (A) Time course of absorbance at 410 nm in the reaction of heme-PM0042 (10 μM) with ascorbic acid (1.0 mM) in 50 mM MES and 150 mM NaCl at pH 6.0 in the absence and presence of 1, 2, 3 and 4 equivalents of Fe^{2+}. (B) Plots of apparent rate constants of heme degradation observed in (A) against concentration of Fe^{2+}.

Heme Degradation Reaction under Multiple Turnover Conditions. Under the premise that the GH repeat sequence captures released iron, the metal binding sites on the sequence should be occupied by Fe^{2+} after several cycles of the reaction. Accordingly, we further examined the heme degradation reaction under multiple turnover conditions. To avoid undesirable degradation of unbound heme by ascorbic acid, 1 equivalent of heme was added after every 30 min. We observed a decrease in the Soret band from 0.88 to 0.48 at 30 min after the reaction. Addition of 1 equivalent of heme led to an increase in Soret absorbance to 0.63, which gradually decreased to 0.48 after 30 min. Addition of ferrozine at this stage did not affect the absorption at 563 nm, indicating that the Fe^{2+}-ferrozine complex was not formed by the addition of 2 equivalents of heme (data not shown). Again, 1 equivalent of heme was added, absorption spectra monitored for 30 min, and the experiment repeated. Finally, ferrozine was added to the solution, which resulted in a band at 563 nm from the Fe^{2+}-ferrozine complex (Figure 8). This band was not observed upon the addition of 2 or 3 equivalents of heme and first appeared in the presence of a total of 4 equivalents of heme. Since ferrozine is an inhibitor of *Vc*HutZ,[12] the compound was not added to the reaction in advance and therefore we could not observe formation of the Fe^{2+}-ferrozine complex in real time. However,

our experiments clearly demonstrate that the GH repeat motif is almost fully occupied by Fe^{2+} released during three cycles of the reaction, which is finally eluted into solvent.

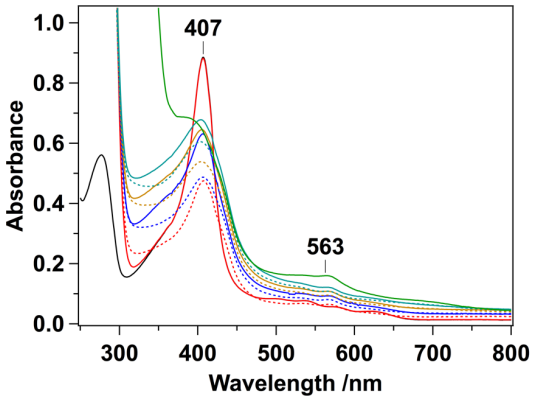

Figure 8. Multiple heme degradation reaction of heme-PM0042 with ascorbic acid (1.0 mM) in 50 mM MES and 150 mM NaCl at pH 6.0. One equivalent of heme was added every 30 min a total of three times. The first, second, third and fourth reaction circles are shown in red, blue, yellow and light blue, respectively. Green line represents spectra following the addition of ferrozine after 4 cycles of the reaction.

Mutational Analysis of the GH Repeat Sequence. To establish the role of the C-terminal GH motif, two truncated mutants lacking residues after positions 171 and 175, respectively, were constructed (Figure S1). Our results showed that neither truncated mutant protein was stable. Notably, addition of heme to the mutants induced aggregation and therefore sufficient amounts of protein could not be obtained for measurements. Next, three histidines within positions 171-175 next to the proximal heme ligand (His169) were substituted with serine (referred to as $(GS)_3$ mutant) (Figure S1) and heme degradation monitored based on disappearance of the Soret band at 407 nm. The absorbance of the $(GS)_3$ mutant decreased with time (Figure S3A). In the presence of 10 μM Fe^{2+}, decrease in absorbance at 410 nm was accelerated, similar to that of WT protein (Figure 6), indicating that metal binding is not influenced by mutation of His171, His173 or His175.

We additionally replaced His177 and His183 of the $(GS)_3$ mutant with threonine (referred to as $(GS)_3$/H177T and $(GS)_3$/H183T, respectively). To avoid too many tandem repeats of nucleotides

derived from glycine and serine residues, threonine was introduced in lieu of serine. The time-course of absorbance changes of the mutants in the absence of Fe^{2+} was almost identical to that of heme-WT PM0042, whereas that in the presence of Fe^{2+} was almost overlapped with that in the absence of Fe^{2+} (Figure S3B, C). This finding supports the possibility that the terminal two histidines in the GH motif contribute to the metal-dependent heme degradation activity of PM0042.

To further confirm the significance of His177 and His183, we constructed two single mutants (H177T and H183T). Unexpectedly, both mutants clearly displayed Fe^{2+}-dependent heme degradation activity (Figure S3D, E). Accordingly, we propose that neither His177 nor His183 contributes solely to metal binding in PM0042, but instead several residues within the GH repeat motif synergistically participate in interactions with metal ions.

Metal Binding to PM0042. Application of isothermal titration calorimetry (ITC) to monitor metal binding to PM0042, revealed no heat accompanying metal binding. This is probably because the exothermic heat of interaction of metal ions with GH repeat sequence would be canceled by the endothermic heat of disruption of the interaction of metal ions with their coordinated-water molecules. Next, metal binding was examined using tryptophan fluorescence. In a previous study, we detected pH-dependent conformational changes of *Vc*HutZ by observing alterations in fluorescence.[3] *Vc*HutZ possesses a sole tryptophan at position 109, which is absent in PM0042. Accordingly, Gly108 of PM0042 corresponding to Trp109 in *Vc*HutZ was replaced with tryptophan. However, this mutant protein could not be successfully expressed. Instead, introduction of tryptophan at position 107 (E107W) generated sufficient amounts of protein for fluorescence measurements, which was subsequently used to evaluate metal binding. Ni^{2+} was utilized in this experiment since prolonged incubation of both PM0042 and heme-PM0042 with metal ions, including Fe^{2+}, caused protein precipitation during titration. Among the metal ions examined, the protein showed the most stable binding to Ni^{2+}. Upon addition of Ni^{2+} to PM0042, fluorescence at

347 nm was decreased (Figure 9A). The intensity changes at 347 nm were further plotted against the concentration of Ni^{2+}. To obtain the apparent dissociation constant, $K_{d,Ni}$, the plot was fitted to Equation 2, which provided a value of 7.0 μM (Figure 9B). The same experiment conducted using heme-PM0042 (Figure 9C) led to an estimated $K_{d,Ni}$ value of ~13.0 μM (Figure 9D). Although the exact dissociation constants of PM0042 for other metal ions were difficult to obtain due to the issue of protein precipitation, values were estimated at ~10 μM.

We measured metal contents of heme-PM0042 using inductively coupled plasma optical emission spectrometer (ICP-OES). Heme-PM0042 contained 1.6 equivalent of Fe^{2+}, which was slightly larger than that we expected of 1.0. After the addition of 1.0 equivalent of Fe^{2+} to the heme-PM0042, followed by removable of unbound Fe^{2+} with a desalting column, the value increased to 2.0. Although the increment of the metal content was 0.4, not 1.0, this result also indicates that metal can bind to heme-PM0042. The same experiment was conducted using Ni^{2+}. The metal contents increased from 0.0 to 0.6 after the treatment of 1.0 equivalent of Ni^{2+}. Some metals were released from the protein during desalting process. Accordingly, we propose that the heme degradation activity of PM0042 is enhanced by Fe^{2+}, but its affinity is relatively low.

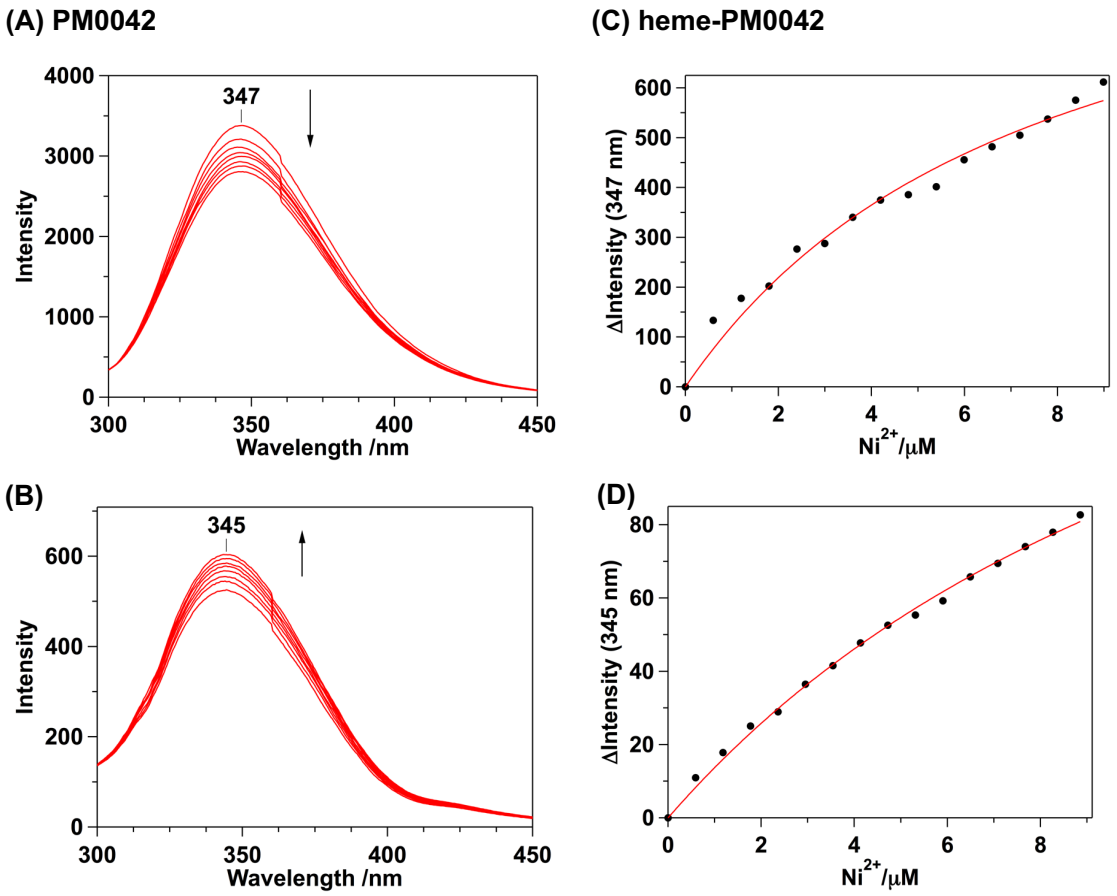

Figure 9. Fluorescence spectral changes of PM0042 (A) and heme-PM0042 (B) following incremental addition of Ni^{2+} (1–30 μM) to PM0042 (10 μM) in 50 mM Tris-HCl and 150 mM NaCl at pH 8.0. Plots of fluorescence at 340 nm against the concentration of Ni^{2+} for PM0042 (C) and heme-PM0042 (D). Solid lines represent fits of the data to Equation 2.

Reduction of Heme-PM0042. To clarify the mechanisms underlying Fe^{2+}-induced enhancement of heme degradation by PM0042, we examined reduction of heme-PM0042 in the absence and presence of Fe^{2+}. Reduction of ferric heme is the initial step of heme degradation using ascorbic acid as the electron donor (Figure S4) and serves as the rate-determining step in the case of *Vc*HutZ.[2] The reduction reaction was completed within a manual mixing time of < 1 s, both in the absence and presence of Fe^{2+}, in significant contrast to *Vc*HutZ, which requires almost 1 h for reduction of heme.[3] Thus, metal-induced heme degradation is not attributable to acceleration of the heme reduction step.

Proton Transfer Process of Heme-PM0042. Another slow step in heme degradation of *Vc*HutZ is protonation of reduced oxyheme (Figure S4).[2,12] Based on the finding that heme degradation by *Vc*HutZ and HO can be slowed down by replacing H_2O with D_2O buffer,[12,19–21] we examined isotope effects on the activity of PM0042. The time courses of absorbance changes at 406 nm for reactions with ascorbic acid in H_2O and D_2O buffer were compared. As shown in Figure 10, heme degradation in D_2O was slower than that in H_2O. The time courses fitted well to a single exponential function and the degradation rate, k_{deg}, was calculated as 0.47 h^{-1} in D_2O, which was lower than that in H_2O by ~3-fold (1.3 h^{-1}). In the presence of 3 equivalents of Fe^{2+}, k_{deg} was increased to 2.0 h^{-1}, which was lower than that in H_2O by ~2-fold (4.2 h^{-1}). These results indicate that protonation is involved in the rate-determining step, which is affected by Fe^{2+}.

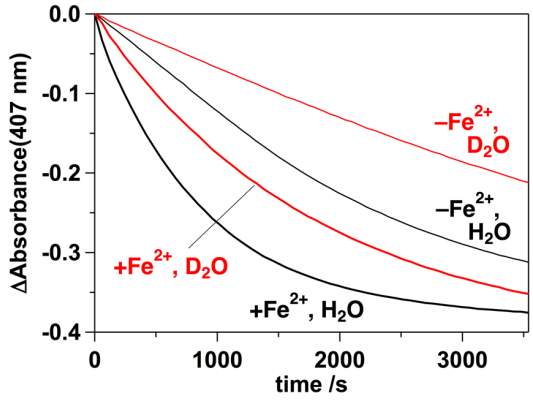

Figure 10. Isotope effect on heme degradation by PM0042 (10 μM). Time course of absorbance changes at 407 nm in the reaction with ascorbic acid (1.0 mM) in H_2O or D_2O buffer at pH 6.0 in the presence and absence of Fe^{2+} (30 μM).

DISCUSSION

Metal-Enhanced Heme Degradation. In view of the homology of PM0042 with *Vc*HutZ (Figure S1), we predicted a similar ability to degrade heme. As expected, heme was degraded by reaction of PM0042 with ascorbic acid (Figure 3). However, the Fe^{2+}-ferrozine complex was not detected upon addition of ferrozine to the solution following the reaction. Considering that reaction

of heme-PM0042 with H_2O_2 produced verdoheme (Figure 3C, D) and HPLC analysis clearly revealed formation of biliverdin (Figure 4C), we conclude that heme is completely degraded by PM0042. In the presence of metal ions, formation of the Fe^{2+}-ferrozine complex was increased (Figure 5), suggesting that Fe^{2+} is released from heme but taken up by the protein. Mutational analyses clearly supported a contribution of the C-terminal GH repeat sequence in capturing Fe^{2+} released from heme (Figure S5).

We hypothesized that the GH repeat sequence should be able to capture divalent metal ions, considering that the His-tag effectively binds to the Ni-nitrilotriacetic acid (NTA) complex. In fact, native PM0042 protein without an additional His-tag yielded an equivalent amount of purified protein using HisTrap column as the N-terminal His_6-tag-fused protein, supporting the theory that the C-terminal GH motif functions to bind metal ions in place of His-tag. The GH repeat sequence is also present in a number of metal transport proteins, such as Co(II)/Ni(II) efflux transporter DmeF (WP_104010668.1) from *Achromobacter xylosoxidans* and zinc transporter 8 from *Drosophila guanche* (GenBank: SPP75815.1), further suggesting that the C-terminal GH motif of PM0042 is capable of metal binding.

The hexahistidine tag (His_6-tag) has high affinity for Ni-NTA (K_d of ~10^{-13} M at pH 8.0).[22] The $K_{d,Ni}$ of PM0042 for Ni^{2+} was estimated as ~10 μM (Figure 9), which was significantly larger than that of His_6-tag, potentially due to the smaller number of histidine residues in the GH repeat sequence. The presence of glycine in place of histidine in the GH motif may contribute to reducing metal affinity, which could be more convenient for sensing of metal concentrations.

Mechanism of Fe^{2+}-Enhanced Heme Degradation. Interestingly, the heme degradation rate was increased ~3-fold in the presence of Fe^{2+} only (Figure 6). *Vc*HutZ displays pH dependence of heme degradation activity, which is derived from the changes in imidazolate characteristics of the

proximal histidine.[3,23] Asp132, a highly conserved residue in the HugZ family, forms a hydrogen bond with His170, whose strength is a determinant of the enzymatic activity of *Vc*HutZ.[3,6] In the case of strong interactions between His170 and Asp132, His170 acquires more imidazolate characteristics, which shifts the redox potential of heme iron to a negative value owing to preference of the oxidized form.[6] Consequently, reduction of heme, the first step of heme degradation, is slower at pH values >8.0.[3,23] At lower pH, these interactions are weakened and the reduced heme yield is significantly increased.

In contrast to *Vc*HutZ, reduction of heme-PM0042 was extremely rapid and thus not a rate-determining step. Consequently, acceleration of this step via binding of Fe^{2+} to the GH repeat does not account for enhancement of the overall heme degradation reaction. Instead, a strong solvent isotope dependence of heme degradation by PM0042 indicates involvement of proton transfer in the rate-determining step (Figure 10). During the heme degradation mechanism of *Vc*HutZ, proton transfer is suggested to occur during conversion step from ferrous oxyheme to hydroperoxy heme (Figure S4).[12] In the case of *Vc*HutZ, iron chelators such as ferrozine and deferoxamine (DFO) disrupt the proton transfer process, leading to significant inhibition of heme degradation activity.[12] The GH repeat sequence of PM0042 attached to the C-terminus (Figure 11, S1) may affect the heme distal and not the proximal site, since proton transfer is assumed to occur at the heme distal region.[24–27] In addition, electron transfer from Fe^{2+} captured by the GH repeat sequence to heme or heme-bound O_2 might be responsible for the Fe^{2+}-enhanced heme degradation. Further studies on metal-induced structural changes of these proteins are required.

Biological Implications of Fe^2-Enhanced Heme Degradation Activity of PM0042. As discussed above, Fe^{2+} interacts with the GH repeat sequence in PM0042 and enhances its heme degradation activity. The affinity of Fe^{2+} for the repeat sequence was estimated as 10 μM (Figure 9). Thus, if the concentration of free labile Fe^{2+} is greater than 10 μM, excess Fe^{2+} binds the repeat

sequence. Under iron-depleted conditions (<10 μM), Fe^{2+} is released from the GH motif and heme degradation reaction slows down, suggestive of a positive feedback mechanism. The presence of glycine in the GH repeat sequence instead of histidine may result in reduced affinity for Fe^{2+}.

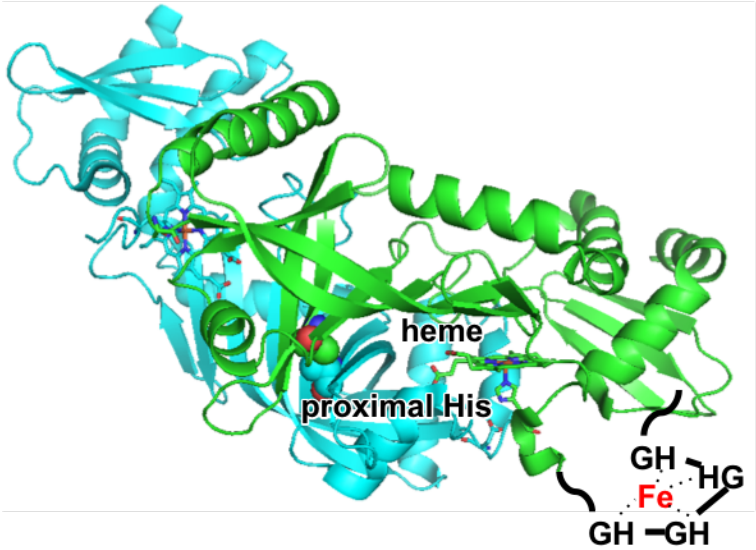

Figure 11. Putative location of GH repeat sequences in PM0042 based on the crystal structure of HugZ (PBD 3GAS).

One possible scenario is that PM0042 activity depends on the environment of *P. multocida*. If Fe^{2+} is enriched in the *P. multocida* environment, heme degradation activity is enhanced to obtain more iron for growth. In contrast, when *P. multocida* exists under low Fe^{2+}conditions, enzymatic activity is suppressed, since the presence of excess iron can be cytotoxic. Therefore, the GH repeat sequence potentially functions as a sensor of metals, particularly Fe^{2+}, for *P. multocida* to control the amount of Fe^{2+} acquired from the environment. This sequence has been identified in a number of metal transporters. The moderate affinity of the GH repeat in PM0042 for metal ions may thus be favorable for the property of metal sensing.

In conclusion, we have demonstrated for the first time that the heme degradation activity of PM0042 is enhanced by Fe^{2+} binding to the GH repeat sequence of the enzyme. In the case of

*Vc*HutZ, the rate-determining step of heme degradation is reduction of heme and changes in the imidazolate character of the proximal histidine are a key regulatory determinant of activity.[2] However, the heme reduction step of heme-PM0042 is extremely rapid relative to that of heme-*Vc*HutZ, indicating that this step is not a rate-determining one. The strong H_2O/D_2O solvent isotope effect on activity suggests that the proton transfer process is a key element in heme degradation by PM0042. Although PM0042 is highly homologous to *Vc*HutZ (except the C-terminal GH repeat sequence), the regulatory mechanisms of the two proteins are distinct. PM0042 is not a metalloenzyme, since the protein does not contain metal cofactors, but metal ions clearly play a key role in regulating its enzymatic activity.

MATERIALS AND METHODS

Materials. Chemicals were purchased from Wako Pure Chemical Industries (Japan), Nacalai Tesque (Japan), Kanto Chemical (Japan) and Sigma-Aldrich (St. Louis, MO) and used without further purification.

Protein Overexpression and Purification. A full-length *pm0042* gene construct (UniProt entry Q9CPJ5) codon optimized for expression in *Escherichia coli* was purchased from Eurofins Genomics (Japan) and amplified via PCR using KOD-Plus-Neo DNA polymerase (Toyobo, Japan) and primers 5'-CCA GGG GCC CCA TAT GAG CGA AGA GCG TCA ACA GA-3' (forward) and 5'-GGA GCT CGA ATT CTC ATT GGT GAC TCG AGG TCT GG-3' (reverse). PCRs were conducted using a MiniAmp Plus thermal cycler (Applied Biosystems), using denaturation temperatures of 98 °C, and annealing and extension temperatures of 68 °C. The amplified fragment was cloned into pET-28b (Merck Millipore, Germany) using a Gibson Assembly kit (New England Biolabs, Beverly, MA). The N-terminal His_6-tag with a thrombin recognition site (Leu-Val-Pro-

Arg-Gly-Ser) in pET-28b vector was deleted to avoid undesirable binding of heme and/or metal ions. The correct gene sequence was confirmed by DNA sequencing (Eurofins Genomics). *E. coli* strains carrying plasmids for *pm0042* were grown at 37 °C in Luria-Bertani (LB) medium supplemented with 50 μg mL^{-1} kanamycin. Expression of protein in *E. coli* was induced with 0.8 mM isopropyl-β-D-thiogalactopyranoside (IPTG) after cell growth reached an optical density at 600 nm (OD_{600}) of 0.6–1.0. The culture was further incubated at 28 °C overnight, cells harvested via centrifugation at 20,000 × g for 5 min and stored at –80 °C until use. The cell pellet was thawed on ice, suspended in lysis buffer (50 mM Tris-HCl, 150 mM NaCl, 0.1% Nonidet P-40, 1 mg mL^{-1} lysozyme and DNase (pH 8.0)) and incubated on ice for a further 60 min. Samples were subsequently centrifuged at 40,000 × g for 30 min and the resulting supernatant loaded onto a HisTrap HP column (Cytiva, Sweden) pre-equilibrated with 50 mM Tris-HCl buffer containing 500 mM NaCl and 20 mM imidazole (pH 8.0). This protein could bind the HisTrap column via an intrinsic histidine cluster without the requirement for an exogenous His_6-tag. The resin was extensively washed (50 mM Tris-HCl, 500 mM NaCl, 50 mM imidazole, pH 8.0) and the bound protein eluted in 50 mM Tris-HCl buffer containing 500 mM NaCl and 200 mM imidazole (pH 8.0).

Mutagenesis was conducted with the aid of a PrimeSTAR mutagenesis basal kit from Takara Bio (Otsu, Japan) and the introduced mutations verified by DNA sequencing (Eurofins Genomics). DNA oligonucleotides were purchased from Eurofins Genomics. The primers for mutagenesis are listed in Table S1 (Supplemental Information). In cases where the histidine residues within the GH repeat sequence were replaced with serine or threonine, the *pm0042* gene was cloned into pGEX-6P-1 (Cytiva) and purified as glutathione S-transferase (GST) fusion protein using COSMOGEL GST-Accept (Nacalai Tesque) owing to loss of the ability of the mutants to bind the HisTrap column. The GST-PM0042 protein was eluted with 10 mM reduced glutathione and 50 mM Tris-HCl (pH

8.0). Eluted GST-fused PM0042 was incubated with human rhinovirus 3C (HRV 3C) protease at 4 °C for ~16 h to remove the GST tag. After cleavage, the reaction mixture was re-applied to the GST-Accept column. The column flowthrough was collected and applied to a HiLoad 16/60 Superdex 200 preparative grade gel filtration column (Cytiva) equilibrated with 50 mM Tris-HCl and 150 mM NaCl, pH 8.0. Protein purity was assessed via sodium dodecyl sulfate-polyacrylamide gel electrophoresis (SDS-PAGE) on a 12.5% polyacrylamide gel.

Measurement of Heme Binding to PM0042. Heme binding was monitored via differential absorption spectroscopy. Successive aliquots of 0.5 mM hemin in 0.1 M NaOH were added to both the sample cuvette containing 10 μM PM0042 and reference cuvette containing buffer alone and spectra recorded 3 min after the addition of each heme aliquot. The absorbance difference at 417 nm was plotted as a function of the heme concentration and dissociation constant ($K_{d,heme}$) calculated using the equation:

$$\Delta A = \Delta A_{max}\left\{[P_t] + [H_t] + K_{d,heme} - \sqrt{\left([P_t] + [H_t] + K_{d,heme}\right)^2 - 4[P_t][H_t]}\right\}/2[P_t] \qquad (1)$$

where ΔA represents the absorption difference between sample and reference cells in the presence and absence of hemin, ΔA_{max} the maximum absorption difference upon addition of hemin, and $[P_t]$ and $[H_t]$ the total protein and hemin concentrations, respectively.

Heme Degradation Activity. The heme degradation reaction of PM0042 was monitored via spectrophotometry (V-660, Jasco, Japan). Briefly, 1.9 mL hemin-reconstituted protein solution (final concentration, 3 μM) in 50 mM Tris-HCl and 150 mM NaCl (pH 8.0) was placed in a cuvette and the reaction initiated by adding 100 μL of 4 mM H_2O_2 or 20 mM ascorbic acid in the same buffer at 25 °C. Spectra were recorded at 1 min intervals for 15 min for H_2O_2 and 2 min intervals for 60 min for ascorbic acid. In reactions with ascorbic acid (final concentration, 1 mM), 1 mg mL^{-1} bovine liver catalase was added to suppress H_2O_2. After completion of the reaction, ferrozine

(Dojindo, Japan) was added to a final concentration of 1 mM. The amount of released iron was calculated by measuring absorbance at 562 nm using an extinction coefficient (ε_{562}) of 27.9 mM^{-1} cm^{-1} [5].

HPLC Analysis of Biliverdin. Heme degradation was induced by incubating a solution of heme-PM0042 (5 μM) in 50 mM Tris-HCl and 150 mM NaCl (pH 8.0) with 0.1 mM H_2O_2 for 30 min at room temperature, followed by the addition of 1 mM ascorbic acid. The reactant was purified using a Supelclean LC-18 solid phase extraction column (Sigma-Aldrich). To extract biliverdin products, a few drops of 1 M hydrochloric acid were added before extraction of the reaction mixture with methanol.

Biliverdin products were analyzed on a HPLC system (LC-2000, JASCO) equipped with a ZORBAX Extend-C18 column (3.0 × 150 mm, 3.5 μm; Agilent Technologies, Santa Clara, CA, USA). Solvents A and B were 10 mM ammonium acetate and methanol, respectively. The running conditions were as follows: flow rate, 1.0 mL min^{-1}; 30% B for 5 min, 30–70% B in 0.1 min, 70–95% B in 25 min, 95% B for 7 min, 95–30% B in 1 min, and 30% B for 20 min. The eluent was monitored at 380 nm. Standards of biliverdin dimethyl esters were prepared as reported elsewhere [28].

Heme Reduction. Reduction of heme was monitored based on changes in absorbance at 418 nm. Ferric heme-PM0042 (5 μM) was reduced by 1 mM ascorbic acid under anaerobic conditions. Although an oxygen scavenging system composed of glucose, glucose oxidase and catalase was added to the solution to maintain anaerobiosis [29], the reaction was conducted under a carbon monoxide (CO) atmosphere to prevent oxidative cleavage of heme and/or autoxidation by contaminated O_2.

Metal titration. Fluorescence spectra were recorded between 300 and 450 nm at a 295 nm

excitation wavelength and scan speed of 200 nm min^{-1} using a FP-8500 spectrofluorometer (JASCO) at excitation and emission slit widths of 5 and 10 nm, respectively. The sample concentration was 3 μM in 50 mM Tris-HCl and 150 mM NaCl (pH 8.0). Each spectrum represents integrated spectra from three consecutive scans.

Fluorescence intensity at 329 nm was plotted against the concentration of metal ions. The metal dissociation constant, $K_{d,M}$, was calculated using the following equation:

$$F = F_0 + \Delta F \left\{ [P_t] + [M_t] + K_{d,M} - \sqrt{\left([P_t] + [M_t] + K_{d,M}\right)^2 - 4[P_t][M_t]} \right\} / 2[P_t] \qquad (2)$$

where F is the fluorescence intensity at a given metal concentration, F_0 the fluorescence intensity in the absence of metal, ΔF the changes in fluorescence intensity upon addition of metal, and $[P_t]$ and $[M_t]$ the total protein and metal concentrations, respectively.

The concentrations of metals attached to heme-PM0042 were measured using an inductively coupled plasma optical emission spectrometer (ICP-OES; ICPE-9000, Shimazu, Kyoto Japan) at emission wavelengths of 238.204, 239.562, 259.939, 273.955 for Fe^{2+} and 221.648, 231.604 for Ni^{2+}. Commercially available mixed-metal standards (Kanto Chemical) were used to construct a standard curve.

ASSOCIATED CONTENT

Supporting Information

The Supporting Information is available free of charge on the ACS Publications website at DOI:

Sequence comparison, mass spectra of reactants, time course of heme degradation of mutant PM0042, and heme degradation mechanism (PDF)

Accession Codes

The UniProt accession ID for PM0042 is Q9CPJ5.

AUTHOR INFORMATION

Corresponding Author

*Department of Chemistry, Faculty of Science, Hokkaido University, Sapporo 060-0810, Japan. E-mail: uchida@sci.hokudai.ac.jp

Authors

Takeshi Uchida

Department of Chemistry, Faculty of Science, Hokkaido University, Sapporo 060-0810, Japan; Graduate School of Chemical Sciences and Engineering, Hokkaido University, Sapporo 060-8628, Japan; orcid.org/0000-0001-9270-8329

Kazuki Ota

Graduate School of Chemical Sciences and Engineering, Hokkaido University, Sapporo 060-8628, Japan

Akinobu Tatsumi

Graduate School of Chemical Sciences and Engineering, Hokkaido University, Sapporo 060-8628, Japan

Syo Takeuchi

Department of Chemistry, School of Science, Hokkaido University, Sapporo 060-0810, Japan

Koichiro Ishimori

Department of Chemistry, Faculty of Science, Hokkaido University, Sapporo 060-0810, Japan; Graduate School of Chemical Sciences and Engineering, Hokkaido University, Sapporo 060-8628, Japan; orcid.org/0000-0002-5868-0462

Notes

The authors declare no competing financial interest.

AUTHOR INFORMATION

We thank the Open Facility, Global Facility Center, Creative Research Institution, Hokkaido University for allowing us to conduct the analysis of metal content using ICPE-9000. We would like to express our gratitude to Ms. Nozomi Takeda (Open Facility Division, Global Facility Center, Creative Research Institution, Hokkaido University) and Kazuyoshi Muranishi (Hokkaido University) for ICP-OES measurement and expertise that greatly assisted the research.

Funding

This research was supported by JSPS KAKENHI Grant Number JP16K05835, JP20K05700

(T.U.) and JP19H05769 (K.I.).

References

(1) Uchida, T., Sekine, Y., Matsui, T., Ikeda-Saito, M., and Ishimori, K. (2012) A heme degradation enzyme, HutZ, from *Vibrio cholerae*. *Chem. Commun. 48*, 6741–6743.

(2) Uchida, T., Sekine, Y., Dojun, N., Lewis-Ballester, A., Ishigami, I., Matsui, T., Yeh, S.-R., and Ishimori, K. (2017) Reaction intermediates in the heme degradation reaction by HutZ from *Vibrio cholerae*. *Dalton Trans. 46*, 8104–8109.

(3) Uchida, T., Ota, K., Sekine, Y., Dojun, N., and Ishimori, K. (2019) Subunit–subunit interactions play a key role in the heme-degradation reaction of HutZ from *Vibrio cholerae*. *Dalton Trans. 48*, 3973–3983.

(4) Gibbs, C. R. (1976) Characterization and application of ferrozine iron reagent as a ferrous iron indicator. *Anal. Chem. 48*, 1197–1201.

(5) Stookey, L. L. (1970) Ferrozine–A new spectrophotometric reagent for iron. *Anal. Chem. 42*, 779–781.

(6) Uchida, T., Dojun, N., Sekine, Y., and Ishimori, K. (2017) Heme proximal hydrogen bonding between His170 and Asp132 plays an essential role in the heme degradation reaction of HutZ from *Vibrio cholerae*. *Biochemistry 56*, 2723–2734.

(7) Goodin, D. B., and McRee, D. E. (1993) The Asp-His-Fe triad of cytochrome *c* peroxidase controls the reduction potential, electronic structure, and coupling of the tryptophan free radical to the heme. *Biochemistry 32*, 3313–3324.

(8) Poulos, T. L. (1993) Peroxidases. *Curr. Opin. Biotechnol. 4*, 484–489.

(9) Gajhede, M., Schuller, D. J., Henriksen, A., Smith, A. T., and Poulos, T. L. (1997) Crystal structure of horseradish peroxidase C at 2.15 Å resolution. *Nat. Struct. Biol. 4*, 1032–1038.

(10) Boyce, J. D., Harper, M., Wilkie, I. W., and Adler, B. (2010) Pasteurella, in *Pathogenesis of bacterial infections of animals* (Gyles, C. L., Prescott, J. F., Songer, J. G., and Thoen, C. O., Eds.) 4th ed., pp 325–346. Blackwell Publishing, Ames, IA.

(11) Liu, Y., Koenigs Lightning, L., Huang, H., Moënne-Loccoz, P., Schuller, D. J., Poulos, T. L., Loehr, T. M., and Ortiz de Montellano, P. R. (2000) Replacement of the distal glycine 139 transforms human heme oxygenase-1 into a peroxidase. *J. Biol. Chem. 275*, 34501–34507.

(12) Dojun, N., Sekine, Y., Ishimori, K., and Uchida, T. (2017) Iron chelators inhibit the heme-degradation reaction by HutZ from *Vibrio cholerae*. *Dalt. Trans. 46*, 5147–5150.

(13) Matsui, T., Unno, M., and Ikeda-Saito, M. (2010) Heme oxygenase reveals its strategy for

catalyzing three successive oxygenation reactions. *Acc. Chem. Res. 43*, 240–247.

(14) Kikuchi, G., Yoshida, T., and Noguchi, M. (2005) Heme oxygenase and heme degradation. *Biochem. Biophys. Res. Commun. 338*, 558–567.

(15) Ortiz de Montellano, P. R. (1998) Heme oxygenase mechanism: Evidence for an electrophilic, ferric peroxide species. *Acc. Chem. Res. 31*, 543–549.

(16) Matsui, T., Nakajima, A., Fujii, H., Matera, K. M., Migita, C. T., Yoshida, T., and Ikeda-Saito, M. (2005) O_2- and H_2O_2-dependent verdoheme degradation by heme oxygenase: Reaction mechanisms and potential physiological roles of the dual pathway degradation. *J. Biol. Chem. 280*, 36833–36840.

(17) Petryka, Z., Nicholson, D. C., and Gray, C. H. (1962) Isomeric bile pigments as products of the in vitro fission of hæmin. *Nature 194*, 1047–1048.

(18) Sakamoto, H., Omata, Y., Adachi, Y., Palmer, G., and Noguchi, M. (2000) Separation and identification of the regioisomers of verdoheme by reversed-phase ion-pair high-performance liquid chromatography, and characterization of their complexes with heme oxygenase. *J. Inorg. Biochem. 82*, 113–121.

(19) Aikens, J., and Sligar, S. G. (1994) Kinetic solvent isotope effects during oxygen activation by cytochrome P-450cam. *J. Am. Chem. Soc. 116*, 1143–1144.

(20) Hallén, S., and Nilsson, T. (1992) Proton transfer during the reaction between fully reduced cytochrome *c* oxidase and dioxygen: pH and deuterium isotope effects. *Biochemistry 31*, 11853–11859.

(21) Davydov, R., Matsui, T., Fujii, H., Ikeda-Saito, M., and Hoffman, B. M. (2003) Kisotope effects on the rate-limiting step of heme oxygenate catalysis indicate concerted proton transfer/heme hydroxylation. *J. Am. Chem. Soc. 125*, 16208–16209.

(22) Schmitt, J., Hess, H., and Stunnenberg, H. G. (1993) Affinity purification of histidine-tagged proteins. *Mol. Biol. Rep. 18*, 223–230.

(23) Uchida, T., Dojun, N., Ota, K., Sekine, Y., Nakamura, Y., Umetsu, S., and Ishimori, K. (2019) Role of conserved arginine in the heme distal site of HutZ from *Vibrio cholerae* in the heme degradation reaction. *Arch. Biochem. Biophys. 677*, 108165.

(24) Unno, M., Matsui, T., and Ikeda-Saito, M. (2007) Structure and catalytic mechanism of heme oxygenase. *Nat. Prod. Rep. 24*, 553–570.

(25) Lad, L., Wang, J., Li, H., Friedman, J., Bhaskar, B., Ortiz de Montellano, P. R., and Poulos, T. L. (2003) Crystal structures of the ferric, ferrous, and ferrous-NO forms of the Asp140Ala

mutant of human heme oxygenase-1: Catalytic implications. *J. Mol. Biol. 330*, 527–538.

(26) Sugishima, M., Moffat, K., and Noguchi, M. (2012) Discrimination between CO and O_2 in heme oxygenase: Comparison of static structures and dynamic conformation changes following CO photolysis. *Biochemistry 51*, 8554–8562.

(27) Fujii, H., Zhang, X., Tomita, T., Ikeda-Saito, M., and Yoshida, T. (2001) A role for highly conserved carboxylate, aspartate-140, in oxygen activation and heme degradation by heme oxygenase-1. *J. Am. Chem. Soc. 123*, 6475–6484.

(28) Wang, J., Lad, L., Poulos, T. L., and Ortiz de Montellano, P. R. (2005) Regiospecificity determinants of human heme oxygenase: Differential NADPH- and ascorbate-dependent heme cleavage by the R183E mutant. *J. Biol. Chem. 280*, 2797–2806.

(29) Englander, S. W., Calhoun, D. B., and Englander, J. J. (1987) Biochemistry without oxygen. *Anal. Biochem. 161*, 300–306.

Graphical abstract

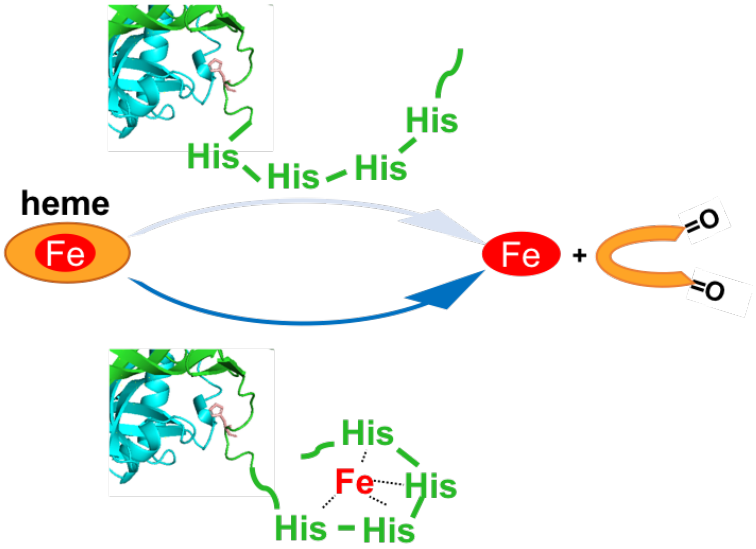

Synopsis

PM0042 from *Pasteurella multocida* is a protein homologous to the heme-degrading enzyme HutZ. PM0042 possesses a glycine-histidine (GH) repeat sequence at the C-terminal region. When Fe^{2+} binds to the GH repeat sequence, heme degradation rate was accelerated by ~3-fold.